

TOWARDS GLOBAL MAPPING OF IRRIGATED AGRICULTURE

M. Ozdogan^{a,*} and G. Gutman^b

^a NASA/GSFC, Mail Code 614.3, Greenbelt, MD, 20771, USA - ozdogan@hsb.gsfc.nasa.gov

^b NASA/HQ, 300 E Street SW, Washington D.C., 20546, USA - ggutman@nasa.gov

KEY WORDS: Irrigation, MODIS, Land-use/Land-cover, Agriculture, Water

ABSTRACT:

We developed an irrigation mapping methodology that relies on remotely sensed inputs from MODerate Resolution Imaging Spectroradiometer (MODIS) instrument, globally extensive ancillary sources of gridded climate and agricultural data and on an advanced image classification algorithm. In the first step, we used climate-based indices of surface moisture status and a map of cultivated lands to provide potential, *first-cut* at global irrigation. To detect actual irrigation, in the second step, we used spatio-temporal and spectral signatures from MODIS remotely sensed data. In particular, we explored three types of irrigation-related indices: i) *Annual* – where we exploited the difference in annual greenness variability between irrigated and non-irrigated crops and related this difference to precipitation availability; ii) *Spectral* – where we exploited a vegetation index (Green Ratio Index) that is sensitive to chlorophyll content; and iii) *Inter-annual* – where we explored the differences in inter-annual changes in vegetation greenness associated with precipitation between irrigated and non-irrigated crops. In the third step, we combined our potential irrigation dataset, remotely sensed indices, and training examples within a supervised classification tool based on a non-parametric decision-tree algorithm to make a binary (i.e. irrigated vs. non-irrigated) irrigated agriculture map. A test of irrigation mapping procedure in a pilot study over the continental US produced a high spatial resolution (1 km) map of irrigated areas with better than 80 percent map accuracy and expected spatial patterns such as a strong east-west divide with most irrigated areas concentrated on the arid west along dry lowland valleys. Future improvements of the method will include estimation of sub-pixel presence of irrigation using remotely-sensed skin temperature measurements.

1. INTRODUCTION

1.1 Motivation and Objective

Accurate information on irrigation extent is fundamental to many aspects of the Earth Systems Science and global change research. These include modeling of water exchange between the land surface and atmosphere, analysis of the impact of climate change and variability on irrigation water requirements/supply, and management of water resources that affect global food security. However, the current extent of irrigated areas over continental to global scales is still uncertain and available maps are derived primarily from country level statistics and maps that are often outdated. Even in locations, such as the US, where the general extent of irrigated areas is known, irrigation-related information exists only in disparate datasets and cannot be easily synthesized into a single continental scale database.

To overcome these limitations, our objective is to develop a methodology to map irrigated agriculture globally with data from the Moderate Resolution Imaging Spectroradiometer (MODIS) instrument at 1-km spatial resolution and ancillary data on climate. Our irrigation mapping methodology is objective, it uses contemporary data, it is robust enough to handle complex forms of irrigation that occur around the globe, and can be repeated across space and time. This irrigation mapping effort is part of our larger research program to understand anthropogenic effects, specifically that of irrigation on global water and energy cycles, climate, agricultural productivity, and agricultural water sustainability. In this paper, we present the methodology and give an example from the Continental US.

1.2 Existing Datasets on Global Irrigation

Currently, there are three global irrigated area products with varying degrees of quality and accuracies. While such datasets have obvious limitations such as being outdated and relatively coarse resolution, they represent the state of the knowledge for the extent of irrigated areas over large geographic regions. The first one of these is the FAO Global Map of Irrigation Areas (GMIA) developed by Döll and Siebert (1999) who combined heterogeneous information on the (approximate) location of irrigated areas with information on the total irrigated area from national and international sources to generate the first global “irrigated lands” map (Figure 1a). The map is a digital raster product with 5-min. spatial resolution and for each cell contains information on the percentage of area *equipped for irrigation* over the period between 1995 and 1999. The map of Döll and Siebert (1999) has become the *de facto* present-day information source for spatial distribution of global irrigated areas although its quality is highly dependent on the national and sub-national data sources used in its making (Figure 1b).

The second product was developed by the Remote Sensing and GIS group at the International Water Management Institute (IWMI) as the Global Irrigated Area Map (GIAM). This dataset has been produced using AVHRR NDVI and Land Surface Temperature data *ca.* 1999 augmented with additional information from SPOT *Vegetation*, JERS-1, and Landsat GeoCover 2000 data, mapped into 10-km grid resolution. (Thenkabail et al, 2005). The Beta release of this product has 53 irrigated classes, derived from the 628 classes in the master file.

Finally, the third product is a sub-product of the USGS Global Land Cover Map (Loveland et al., 2000). Under the auspices of the IGBP-DIS (International Geosphere Biosphere Programme-Data and Information System), a global land-cover database

* Corresponding author.

was generated based on 1-km AVHRR observations received during the period April 1992 through September 1993. The USGS global land-cover data set includes several legends, all

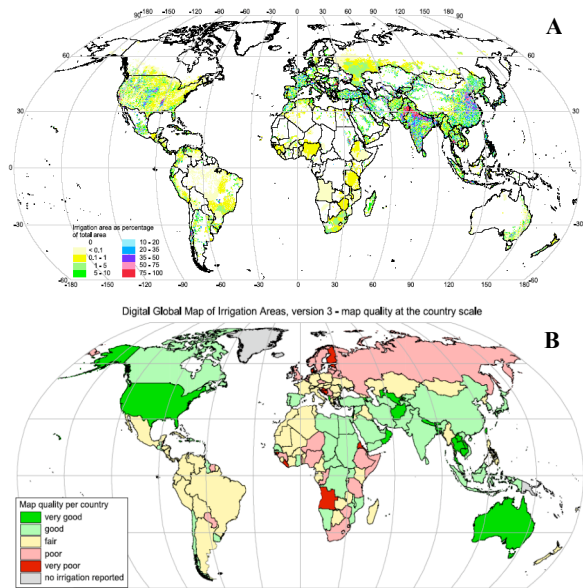


Figure 1. A) Global Map of Irrigation Areas (GMIA) shown as percentage of each 5min cell obtained using FAO country reports and other ancillary data; B) GMIA per country quality.

based on the same database (Loveland et al., 2000). Of these, the Global Ecosystems Legend contains four classes defined as irrigated land: *irrigated grassland, rice paddy and field, hot irrigated cropland, and cool irrigated cropland*. When combined, these classes provide one of the few sources of remotely sensed information on spatial distribution of irrigation at global scales.

While these data sources provide the best available source of information regarding the distribution of irrigation at global scales they also suffer from serious shortcomings. For example, the Doll and Siebert map (GMIA) primarily represents the areas *equipped to be irrigated circa* 1995-2000. However, the irrigated agricultural lands are extremely dynamic, driven by each year's precipitation availability, the choice of crop type, and the ability to irrigate on the farmers end. Moreover, the irrigated areas were determined from disparate data sources, primarily at the county level, the sub county information is less reliable. For example, a comparison of this product to the other mentioned products over Mexico where it is said to have low reliability (according to Figure 1b above) reveals stark differences and relative omission/commission errors (Figure 2-middle). The major shortcoming of the USGS map is that irrigated areas were determined as part of a broader classification scheme, not just irrigation. Thus the emphasis was primarily placed on other land cover types and thus irrigated classes has received less attention and decreased classification accuracy. A recent comparison by Vorosmarty (2002) of irrigated lands depicted by the USGS map to the country-level reports of irrigated area points to major uncertainties in the capacity to classify and inventory irrigated lands due to highly politicized nature of FAO data reports as well as technical limitations of the more objective geophysical datasets. This deficiency is also revealed in Figure 2-top. Likewise the major drawback of the IWMI global irrigation map product (GIAM) is that ground-truth data obtained only in India, SE Asia, Africa, and South America were used to adjust

and refine global irrigation classes. This makes the IWMI product highly parameterized per region for which extensive ground data exists. Over areas without such data and over the entire globe, the irrigation classes are rather less reliable (Figure 2-bottom).

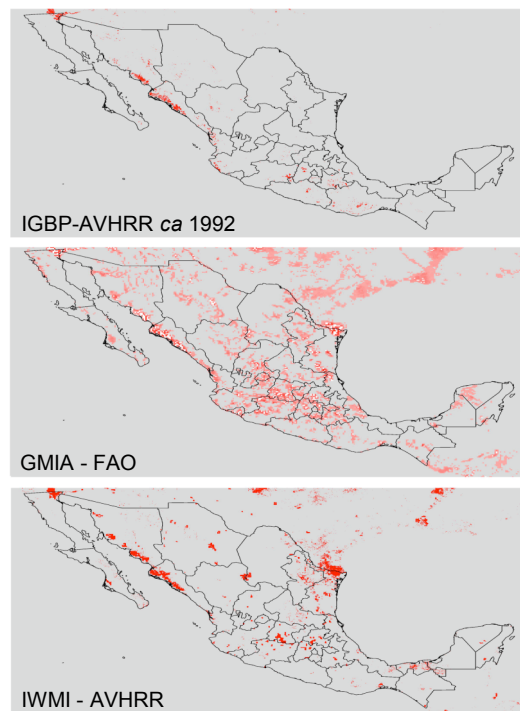


Figure 2. Comparison of three global irrigation products over Mexico. As shown, the GLCC dataset (top) has large omission errors while the other two datasets have both relative omission/commission errors.

2. IRRIGATION MAPPING METHODOLOGY

2.1 Overview

As part of our objective to map irrigated lands globally, our proposed irrigation mapping procedure meets several important criteria. First, the procedure is automated and repeatable across space and time. Second, it is robust enough to capture many different forms of irrigated lands across large geographic regions. Third, it relies on high quality and objective remotely sensed observations. To meet these criteria, we take an image classification approach to irrigation mapping problem. While the intent is irrigation mapping, the fundamental process is image classification of remotely sensed, multi-temporal, multi-spectral images, guided by a climate index specifically suited for irrigation presence.

Our irrigation mapping procedure has three major parts that are schematically shown in Figure 3. In the first part, we calibrate a climatological moisture (or dryness) index along with existing agricultural maps to define irrigation potential. In the second part, we identify irrigation-related remotely sensed temporal and spectral indices. In the third and final part, we combine irrigation potential and remotely sensed indices within a supervised classification algorithm to locate irrigation at moderate spatial resolution (500m – 1000m). We initially tested our procedure in the US to map irrigated lands across the entire country. Our preliminary results from this first implementation of the procedure are extremely encouraging and warrant pursuing in other locations around globe. In the sections

that follow, we describe the steps our procedure in greater detail. In the last section, we show the first examples from the US.

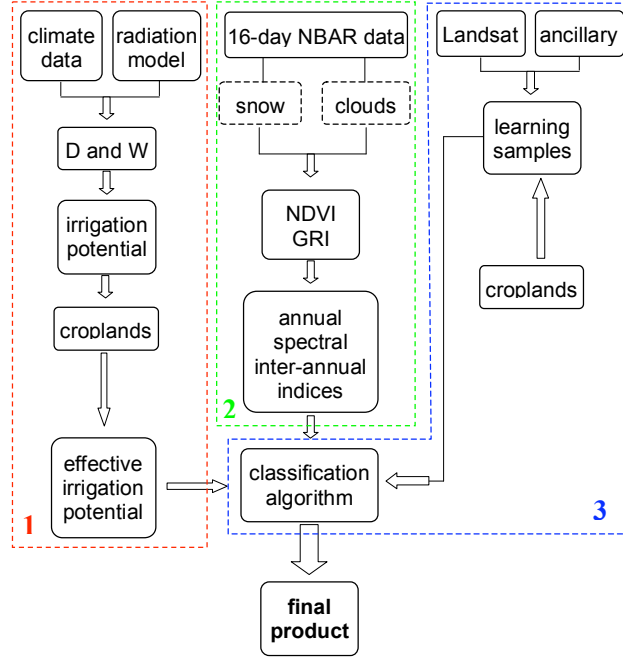


Figure 3. Schematic representation of the proposed irrigation mapping procedure.

2.2 Effective Irrigation Potential

Irrigation is practiced in most countries at scales ranging from small subsistence farming to national enterprises. But the actual location is determined by a combination of factors including climate, resource availability, crop patterns, and technical expertise. Climate plays an important role in presence and distribution of irrigation as it determines natural moisture availability (precipitation), crop water demand (evaporation), and crop schedules. In this study, we developed a climate-based index for outlining potentially irrigated areas. A map of potentially irrigated areas in the form of a climate-based index provides the first approximation for areas that potentially require irrigation, which we further refine using remote sensing data.

Over large areas, presence and distribution of irrigation is primarily controlled by natural moisture availability at the surface. For example, in arid and semi-arid parts of the world, dry atmosphere and the lack of rain-supplied moisture requires exclusive use of irrigation to grow crops. In more humid locations, on the other hand, irrigation, if necessary at all, is often in the form of supplemental irrigation, meeting the excess demand of crops whose growth cycle is out of sync with natural precipitation. Thus, climatic moisture availability (or dryness) provides the first level of information on potential presence of irrigation at a given location.

One index that provides suitable information on surface moisture status and the geobotanic state is the *Radiative Dryness Index* proposed by Budyko (1974):

$$D = \frac{R}{\lambda P} \quad (1)$$

where R is mean annual net radiation, which we estimated from Earth-Sun geometry, observed mean air temperature, and observed humidity; P is mean observed annual precipitation; and λ is latent heat of vaporization. The dryness ratio has been widely used to classify climate regimes and corresponding land cover in simple climate models (e.g. Gutman et al., 1984). While D provides important information on climatic moisture availability, it is not directly related to irrigation. To relate the D to irrigation, we plotted D against percent irrigation presence information from the GMIA product (Siebert et al, 2005). This relationship is shown in Figure 4 as black open circles (original aggregated data) and a black curve (fitted). While the relationship between D and fractional irrigated area show some expected patterns, the curvilinear nature of the relationship is hard to interpret. To relate dryness characterized by D to the *Water Availability Parameter*, Gutman et al (1984) used the empirical relationship suggested by Lettau (1969):

$$W = \frac{\tanh D}{D}, \quad D \geq 0 \quad (2)$$

The relationship between W and fractional irrigated area is given in Figure 4 by a linear fit of the original aggregated data.

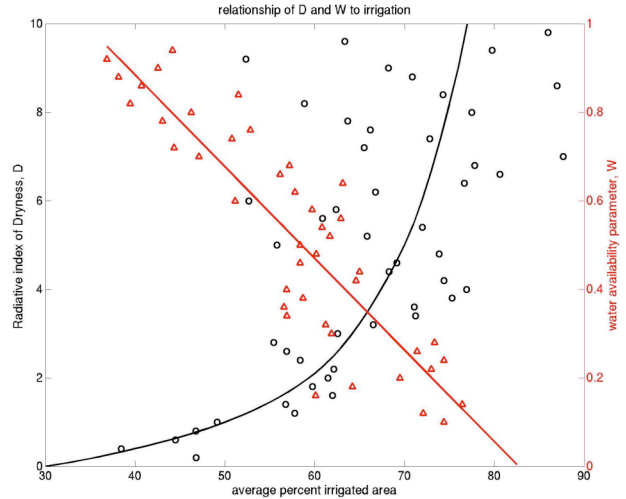


Figure 4. The relationship between D , W , and global fractional irrigated area obtained from the GMIA product. D is plotted as circles and the fitted curve, while W is plotted as triangles and the straight fitted line. Note that W linearizes the relationship between D and irrigated area and thus it is used to map irrigation potential.

Using this linear relationship between W and fractional irrigated area, we mapped climate-based irrigation potential. The darkest areas in Figure 5a show highest potential for irrigation based solely on climate. Since we are ultimately interested in irrigated croplands, we further refined this map by masking out areas that are known to be not cultivated (Ramankutty and Foley, 1996) (Figure 5b). We call this final masked product the effective irrigation potential map and it shows some expected patterns. For example, while the entire Australian continent has a very high irrigation potential due to generally dry climate of the region, only cultivated lands along the southeast and southwest corners of the country have high effective irrigation potential.

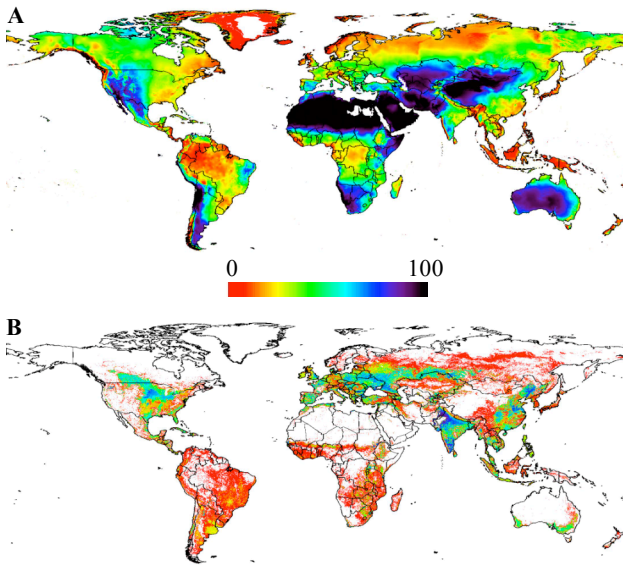


Figure 5. Effective Irrigation Potential (B) created by crop masking the original irrigation potential map (A) developed by relating W to irrigation presence.

In our irrigation mapping procedure, we used effective irrigation potential as ancillary information in the classification process, which has generally resulted in improved classification accuracies of remotely sensed images (Strahler, 1980; McIver and Friedl, 2002).

2.3 Remote Sensing of Irrigation

The effective irrigation potential map shows areas that are potentially irrigated. These areas may not always coincide with areas that are actually irrigated, which is due to infrastructure and water availability. To map actual irrigation, we used remotely sensed indices based on data from the MODIS sensor.

MODIS Data

The MODIS sensor includes seven spectral bands that are designed exclusively for monitoring Earth's land surfaces. The MODIS instrument is located on-board both Terra and Aqua platforms, and when combined, provides at least twice-daily global coverage at 250- and 500-m spatial resolutions. Compared to the heritage AVHRR instrument, the MODIS data offers enhanced spectral, spatial, radiometric, and geometric quality for improved mapping and monitoring of vegetation activity. Hence, to date, MODIS land data has been an integral part of production of a large variety of land cover maps, including irrigation (Friedl et al., 2002; Thenkabail, et al., 2005; Xiao et al., 2006).

A large array of standard MODIS data products are operationally produced by the MODIS Land Science Team and made available to the scientific community on a timely basis. One of these products is the Nadir BRDF-adjusted Reflectance (NBAR) data (MOD34B4) (Schaaf et al., 2002). This product provides cloud-screened and atmospherically corrected surface reflectances for all MODIS land bands that have been corrected for view- and illumination-angle effects. This angular correction substantially reduces the source of noise related to surface and atmospheric anisotropy. Currently, the NBAR data is produced at aggregated 1 km spatial resolution, every 16 days with a total of 23 observations over the calendar year,

geographically organized in a MODIS tile system with the Sinusoidal Projection. In this study we used 2 calendar years (2002/2003) of NBAR data (total of 46 observations).

2.3.2 Irrigation-related Indices

Remote sensing of irrigated lands over large geographic regions involves significant challenges in terms of both selecting spectral bands or indices that contain maximum amount of irrigation related information and relating this information to complex forms of irrigation presence.

To determine actual irrigation presence we identified spatio-temporal patterns of vegetation greenness from remotely sensed data. In particular, we have identified three types of irrigation-related signatures. These signatures are: 1) *Annual*, we exploit the variability in timing of greenness between irrigated and non-irrigated croplands and precipitation; 2) *Spectral*, we use the Green Ratio Index (GRI) (Gitelson et al 2006) to amplify the signal; and 3) *Inter-annual*, we exploit inter-annual changes in vegetation greenness based on the hypothesis that irrigated lands would have less inter-annual variability as development of those crops does not depend on precipitation.

Annual Indices

There is an overwhelming consensus that the Normalized Difference Vegetation Index (NDVI) is an important vegetation monitoring tool (Tucker, 1979; Goward et al., 1991; DeFries et al., 1998). NDVI is defined as:

$$NDVI = \frac{\rho_{nir} - \rho_{red}}{\rho_{nir} + \rho_{red}} \quad (3)$$

where ρ_{nir} and ρ_{red} respectively represent NIR and red reflectances. NDVI has been closely related to plant moisture availability (Nicholson et al. 1990), leaf area index (Xiao et al. 2002), primary production (Prince, 1991); and vegetation fraction (Gutman and Ignatov, 1998).

While NDVI has been widely used to monitor vegetation greenness in agricultural settings under a variety of climatic conditions, overwhelmingly, it is the temporal NDVI signal that has often been most related to irrigation (Tucker and Gatlin, 1984; Martinez-Beltran and Calera-Belmonte, 2001; Ozdogan et al. 2006). In particular, greenness associated with non-irrigated crops in arid/semi-arid landscapes is often a direct result of rainfall events while greenness associated with irrigated sites is generally independent of rainfall and would show a development cycle completely different than that of rain-fed crops. This differential temporal behaviour of irrigated and non-irrigated cultivations is illustrated in Figure 6 for a relatively arid location in northwestern US where year 2002 vegetation greenness for irrigated (solid) and non-irrigated (dashed) croplands are plotted in the form of mean smoothed NDVI profile (left Y-axis). Also plotted in the same figure is the monthly mean precipitation for the same year (right Y-axis). The non-irrigated crops exhibit two peaks, first following planting in the fall and second before harvest in late spring/early summer, closely following the moisture availability through precipitation. In contrast, irrigated crops peak in greenness during mid-summer when moisture availability is the smallest and greenness value of non-irrigated crops drops to its lowest value. Note that the lack of precipitation in the summer time at this location causes a large moisture deficit and makes irrigation absolutely necessary. In this particular location, the irrigated

and non-irrigated crops exhibit clearly distinct temporal greenness profiles especially when related to precipitation availability and we exploit this annual index in our irrigation mapping procedure.

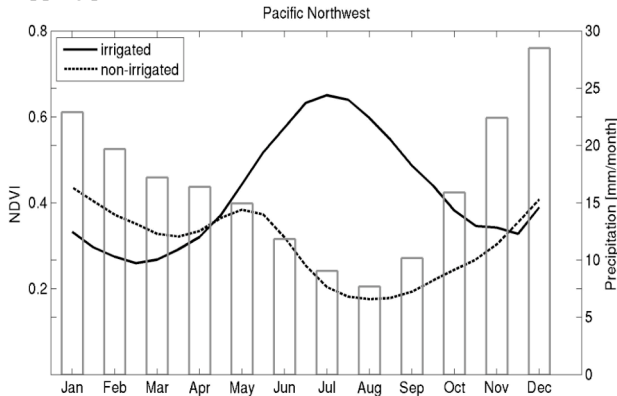


Figure 6. An example annual index in the form of 2002 NDVI profiles for irrigated (solid line) and non-irrigated (dashed line) crops in northwestern US. Also plotted is the monthly precipitation availability. Note that irrigated crops peak in greenness when moisture availability from precipitation is the lowest suggesting irrigation presence.

Spectral Indices

A more difficult case for distinguishing irrigated crops from non-irrigated ones occurs in locations where the same crop type is grown with and without irrigation in the same growing season. Our preliminary work with NDVI in Nebraska, USA suggests that while irrigated fields exhibit slightly larger NDVI than non-irrigated counterparts, possibly due to constant availability of moisture, the difference in NDVI is small and potentially useless in distinguishing irrigated fields. Thus, a more sensitive index is required to make this distinction.

Large body of research into spectral remote sensing of vegetation canopies indicates that moisture stress in vegetation is strongly manifested in spectral indices related to Chlorophyll content (Gitelson et al, 2003). One such index, suggested by Gitelson et al (2006) to be used with the MODIS sensor, is the Green Ratio Index (GRI) defined as:

$$GI = (\rho_{nir} / \rho_{Green}) - 1 \quad (4)$$

where ρ_{green} is the reflectance in green spectral region. The theoretical foundation of the *GRI* is based on the observation that in the green spectrum (centered around 510 nm) specific absorption coefficient of chlorophylls is very low while green leaves absorb more than 80 percent of incident light in this spectral range (e.g., Gitelson and Merzlyak 1994). In contrast, depth of light penetration into leaves in the blue and red spectral ranges is four- to six-fold lower (e.g., Merzlyak and Gitelson, 1994). Therefore, in the green, absorption of light is high enough to provide high sensitivity of *GRI* to Chl content but much lower than in the blue and red to avoid saturation (Gitelson et al., 2003). To demonstrate the sensitivity of *GRI* to irrigation presence, we plotted temporal *GRI* profiles of irrigated (solid line) and non-irrigated (dashed line) maize in Figure 7. While the two temporal profiles are identical in timing of greenness, the absolute values are significantly different, suggesting that soil moisture stress in maize associated with lack of moisture exhibits smaller *GRI* and thus lower Chlorophyll content than irrigated maize.

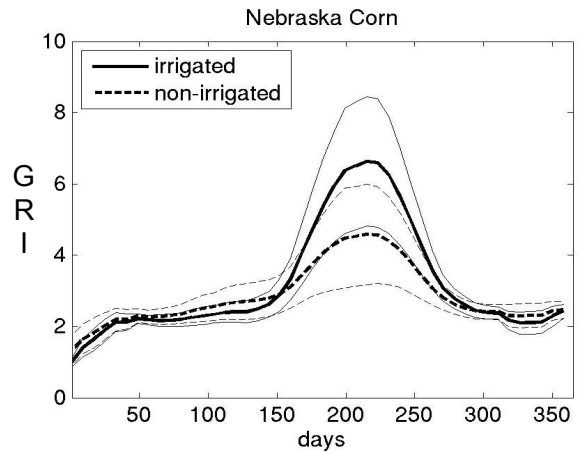


Figure 7. Mean temporal profiles of *GRI* associated with irrigated (solid line) and non-irrigated (dashed line) maize in Nebraska, USA. Note the difference in absolute value of *GRI*. Also plotted is one standard deviation around the mean for each.

Inter-annual Indices

Water available for agricultural crops through precipitation varies significantly across years. In addition to management practices such as fertilizer and tilling, this natural variability of moisture contributes significantly to each year's crop quality and yield that can be monitored from space through vegetation indices. In contrast, the status and quality of croplands that receive significant amounts of irrigation on a regular basis would be expected to be independent of natural precipitation availability as natural water limitation is alleviated by artificial application of water through irrigation. Thus, inter-annual variation in vegetation greenness for irrigated fields would be expected to be less than inter-annual greenness variation of non-irrigated croplands assuming the same crop type is examined across years.

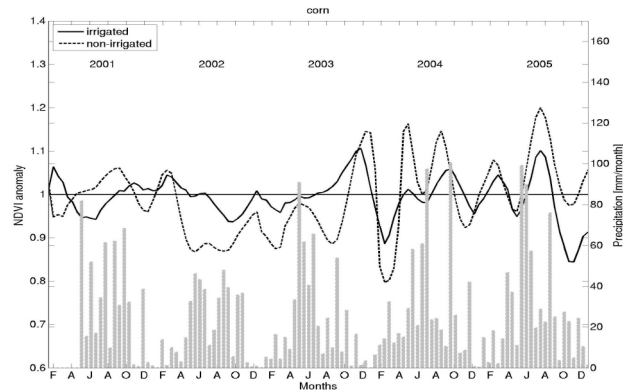


Figure 8. Inter-annual profiles of NDVI anomaly (defined as deviation from 5-year mean) for irrigated and non-irrigated maize in Midwestern US. Also plotted is bi-monthly precipitation.

To test this hypothesis, we analyzed five years of MODIS NDVI data for maize and soybeans in Midwestern US (Figure 8). Analysis of *inter-annual* data suggests that irrigated maize indeed exhibits lower inter-annual variability (shown in Figure 8 as the solid line) than vegetation greenness associated with non-irrigated maize fields (displayed as the dashed curve) which varies significantly across years, following precipitation.

2.4 Classification Algorithm

As our approach to irrigation mapping is a supervised classification methodology, it requires training data that characterizes the desired output classes (irrigation in this case). We derived these training (learning) samples from several dozen high spatial resolution satellite imagery acquired by the Landsat 7 ETM+ sensor *circa* 2000. The location of the training sites were chosen to represent major irrigated land areas of the US and interpreted with the help of ancillary data sources such as county based irrigated area maps as well as based on characteristic shapes of irrigated fields. These training locations were used to extract cloud- and snow-screened high quality examples of the three irrigation related indices representing the annual, spectral, and inter-annual behaviour of irrigated and non-irrigated crops. We then used these sample data as training examples in the learning phase of the decision tree classification algorithm as shown in Figure 3.

3. IMPLEMENTATION IN THE CONTINENTAL US

The first step in our implementation of the irrigation mapping procedure for the Continental US was to screen the MODIS time series data for clouds and snow cover. We used the quality control cloud flags that are included in the NBAR data files in the form of cloud masks for each 16-day time period for a total of 23 files per year. To minimize the potential impact of snow cover, especially in the winter months, we generated snow masks using the Normalized Difference Snow Index (Hall et al., 1995). Pixels corresponding to clouds and snow were then excluded from the analysis. The second step was to train the decision tree model with the example datasets of irrigation indices and effective irrigation potential derived from the training sites described above to automatically generate the rules and thresholds to identify irrigation. We then applied the trained decision tree to all of the individual MODIS tiles that cover the Continental US. Each tile consisted of cloud and snow screened time series of vegetation index values representing a total of 138 per-pixel observations (2 years between 2002 and 2003, 23 observations per year, and 3 vegetation indices). The end result of the classification algorithm was a two-class map showing irrigated and non-irrigated areas over the Continental US (Figure 9).

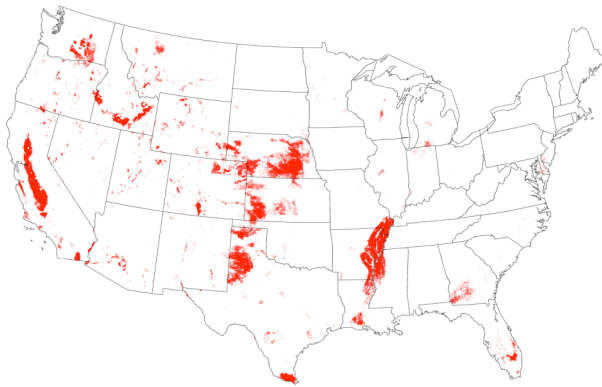


Figure 9. Irrigation in the Continental US *circa* 2002 obtained by implementing the procedure proposed here. The distribution of irrigated lands follows expected patterns. In the arid western portion of the US, irrigation occurs in narrow dry valleys such as the central valley of California. In more humid eastern portion of the US, irrigation occurs along major agricultural provinces.

To qualitatively assess the final irrigation map as a result of our mapping procedure, we compared it to the year 2002 USDA *dot-map* (Figure 10). The USDA *dot-map* was generated by randomly placing a dot for each 5,000 ha of irrigated area in each US county, regardless of the location of irrigation. At the continental scale, this *dot-map* is the only source of information on irrigation presence. Nevertheless, comparison of this *dot-map* to the map generated by implementing our mapping procedure reveals good agreement, suggesting that our proposed methodology is able to capture major irrigation patterns in the continental US. Moreover, it provides additional information on irrigation location, beyond the limits of the standard *dot-map* products.

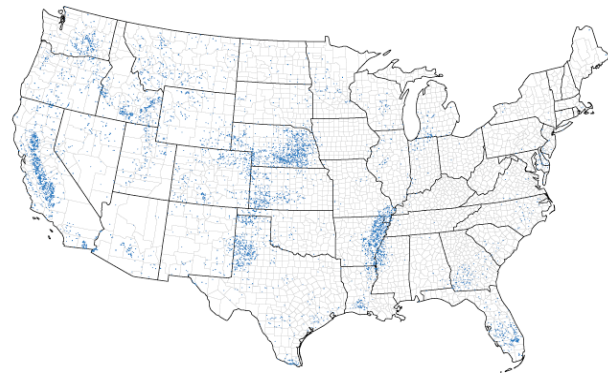


Figure 10. County-based irrigation *dot-map* for the US for the year 2000 obtained from the USDA. The USDA *dot-map* was generated by randomly placing a dot for each 5,000 ha of irrigated area in each US county, regardless of the location of irrigation.

While our preliminary test product is at relatively high spatial resolution (500-1000 m) it may fail to capture sub-pixel presence and variability of irrigation, especially if irrigated fields are much smaller than the spatial resolution of the observing sensor. This issue may be especially important when the proposed methodology is applied to locations (for example in China) where irrigated agricultural fields are known to be small (Ozdogan and Woodcock, 2006). To improve subpixel representation of irrigation, we tested several different subpixel mapping methods and discovered that skin temperature is inversely related to irrigation presence. The future improvements of the proposed procedure will incorporate remotely-sensed skin temperature data to recover subpixel irrigation information once irrigated/non-irrigated pixels have been identified.

References

- Budyko, M.I., 1974. *Climate and Life*. Academic Press, 508 pp.
- DeFries, R.S., Hansen, M., Townshend, J.R.G., and Sohlberg, R., 1998. Global land cover classifications at 8 km spatial resolution: The use of training data derived from Landsat imagery in decision tree classifiers, *Int. J. Remote Sensing*, 19, pp. 3141-3168.
- Döll, P. and Siebert, S., 1999. A digital global map of irrigated areas. Report A9901. Germany: *Center for Environmental systems Research, University of Kassel*.
- Friedl, M.A, McIver, D.K., Hodges, J.C.F., Zhang, X.Y., Muchoney, D., Strahler, A.H., Woodcock, C.E., Gopal, S., Schneider, A., Cooper, A., Baccini, A., Gao, A., and Schaaf, C.;

2002. Global land cover mapping from MODIS: algorithms and early results, *Remote Sensing of Environment*, 83, pp.287:302.
- Gitelson, A.A. and Merzlyak, M.N., 1994. Quantitative estimation of chlorophyll *a* using reflectance spectra: Experiments with autumn chestnut and maple leaves, *J. Photochem. Photobiol. (B)* 22, pp. 247–252.
- Gitelson, A.A., Gritz, U. and Merzlyak M.N. 2003. Relationships between leaf chlorophyll content and spectral reflectance and algorithms for non-destructive chlorophyll assessment in higher plant leaves. *J. Plant. Physiol.*, 160, pp. 271-282.
- Gitelson, A.A., Vina, A., Verma, S.B., Rundquist, D.C., Arkebauer, T.J., Keydan, G., Leavitt, B., Ciganda, V., Burba, G.G., and Suyker, A.E., 2006. Relationship between gross primary production and chlorophyll content in crops: Implications for the synoptic monitoring of vegetation productivity, *Journal of Geophysical Research*, 111, D08S11, doi:10.1029/2005JD006017.
- Goward, S.N., Markham, B., Dye, D., Dulaney, W., and Yang, J., 1991. Normalized difference vegetation index measurements from the advanced very high resolution radiometer, *Remote Sensing of Environment*, 35, pp. 257-277.
- Gutman, G., Ohring, G., and Joseph, J.H., 1984. Interaction between the geobotanic state and climate: A suggested approach and test with a zonal model, *Journal of the Atmospheric Sciences*, 41, pp. 2663-2678.
- Gutman, G. and Ignatov, A., 1998. Derivation of green vegetation fraction from NOAA/AVHRR for use in weather prediction models, *Int. J. Rem. Sens.*, 19, pp. 1533-1543.
- Hall, D. K., Riggs, G. A., and Salomonson, V. V., 1995. Development of methods for mapping global snow cover using moderate resolution imaging spectroradiometer data, *Remote Sensing of Environment*, 54, pp. 127– 140.
- Lettau, H., 1969. Evapotranspiration climatology: A new approach to numerical prediction of monthly evapotranspiration, runoff and soil moisture storage, *Monthly Weather Review*, 97, pp. 691-699.
- Loveland, T.R., Reed, B.C., Brown, J.F., Ohlen, D.O., Zhu, J, Yang, L., and Merchant, J.W., 2000. Development of a Global Land Cover Characteristics Database and IGBP DISCover from 1-km AVHRR Data, *International Journal of Remote Sensing*, 21, pp.1,303-1,330.
- Martinez-Beltran, C. and Calera-Belmonte, A., 2001. Irrigated crop estimation using Landsat TM imagery in La Mancha, Spain, *Photogramm. Eng. Rem. Sen.* 67, pp. 1,177–1,184.
- Nicholson, S.E., Davenport, M.L., and Malo, A.R., 1990, A Comparison of vegetation response to rainfall in the Sahel and East Africa using normalized difference vegetation index from NOAA-AVHRR, *Climatic Change*, 17, pp. 209-241.
- Ozdogan, M., Woodcock, C.E., Salvucci, G.D., and Demir, H., 2006. Changes in summer irrigated crop area and water use in Southeastern Turkey from 1993-2002: Implications for current and future water uses, *Water Resources Management*, 20(3), pp. 467-488.
- Ozdogan, M. and Woodcock, C.E., 2006. Resolution dependent errors in remote sensing of cultivated areas, *Remote Sensing of Environment*, 103: 203-217.
- Prince, S.D., 1991. Satellite remote sensing of primary production: comparison of results for Sahelian grasslands, *International Journal of Remote Sensing*, 12, pp. 1133-1421.
- Ramankutty, N. and Foley, J.A., 1998. Characterizing patterns of global land use: an analysis of global croplands data. *Global Biogeochemical Cycles*, 12(4), pp. 667-685.
- Schaaf 2002 Schaaf, C. B., F. Gao, A. H. Strahler, W. Lucht, X. Li, T. Tsang, N. C. Strugnell, X. Zhang, Y. Jin, J.-P. Muller, P. Lewis, M. Barnsley, P. Hobson, M. Disney, G. Roberts, M. Dunderdale, C. Doll, R. d'Entremont, B. Hu, S. Liang, and J. L., 2002. Privette, First Operational BRDF, Albedo and Nadir Reflectance Products from MODIS, *Remote Sens. Environ.*, 83, pp. 135-148.
- Thenkabail, P.S., Schull, M., and Turrall, H., 2005. Ganges and Indus river basin land use/land cover (LULC) and irrigated area mapping using continuous streams of MODIS data, *Remote Sensing of Environment*, 95, pp. 317-341.
- Tucker, C., 1979. Red and photographic infrared linear combinations for monitoring vegetation, *Remote Sensing of Environment*, 8, pp. 127-150.
- Tucker, C. J. and Gatlin, T.A., 1984. Monitoring vegetation in the Nile Delta with NOAA 6 and NOAA 7 AVHRR imagery. *Photogrammetric Engineering and Remote Sensing*, 50(1), pp. 53 61.
- Vorosmarty, C.J., 2002. Global water assessment and potential contributions from Earth System Science, *Aquat. Sci.*, 64, pp. 328-351.
- Xiao, X., Boles, S., Frohling, S., Salas, W., Moore, B., Li, C., et al., 2002. Observation of flooding and rice transplanting of paddy rice fields at the site to landscape scales in China using VEGETATION sensor data, *International Journal of Remote Sensing*, 23, pp. 3,009– 3,022.
- Xiao, X., Boles, S., Frohling, S., Li, C., Babu, J.Y., Salas, W., and Moore, B., 2006. Mapping paddy rice agriculture in South and Southeast Asia using multi-temporal MODIS images, *Remote Sensing of Environment*, 100, pp. 95-113.